Fast 3-D temporal focusing microscopy using an electrically tunable lens

Jun Jiang,[1] Dapeng Zhang,[1] Steven Walker,[1,2] Chenglin Gu,[1] Ya Ke,[2] Wing Ho Yung,[2] Shih-chi Chen [1,*]

[1]*Department of Mechanical and Automation Engineering and Shun Hing Institute of Advanced Engineering, The Chinese University of Hong Kong, N.T., Hong Kong*
[2]*School of Biomedical Sciences, The Chinese University of Hong Kong, N.T., Hong Kong*
[*] *scchen@mae.cuhk.edu.hk*

Abstract: In this paper, we present a 3-D temporal focusing microscope based on an electrically tunable lens (ETL) and a femtosecond regenerative laser amplifier. The focus-tunable lens provides a fast and compact way to perform non-mechanical z-scanning and resolves the blurry image issue compared with GVD-based z-scanning methods. The optical performance of the temporal focusing system, including z-scanning characteristics, the associated the magnification variation, and the lateral and axial resolution, has been studied and characterized using calibrated Rhodamine-6G thin film sample, fluorescent beads, and pollen samples. Lastly, we demonstrate the optical cross-sectioning and z-scanning capability with an *in vivo* experiment, where Ca^{2+} imaging of neurons in GaCamp6 labeled zebrafish was performed.

OCIS codes: (180.6900) Three-dimensional microscopy; (180.4315) Nonlinear microscopy; (180.2520) Fluorescence microscopy; (170.6900) Three-dimensional microscopy; (170.2520) Fluorescence microscopy

References and links

1. W. Denk, J. H. Strickler, and W. W. Webb, "Two-photon laser scanning fluorescence microscopy," Science **248**(4951), 73–76 (1990).
2. E. J. Botcherby, C. W. Smith, M. M. Kohl, D. Débarre, M. J. Booth, R. Juškaitis, O. Paulsen, and T. Wilson, "Aberration-free three-dimensional multiphoton imaging of neuronal activity at kHz rates," Proc. Natl. Acad. Sci. U.S.A. **109**(8), 2919–2924 (2012).
3. G. Y. Fan, H. Fujisaki, A. Miyawaki, R. K. Tsay, R. Y. Tsien, and M. H. Ellisman, "Video-rate scanning two-photon excitation fluorescence microscopy and ratio imaging with cameleons," Biophys. J. **76**(5), 2412–2420 (1999).
4. Q. T. Nguyen, N. Callamaras, C. Hsieh, and I. Parker, "Construction of a two-photon microscope for video-rate Ca2+ imaging," Cell Calcium **30**(6), 383–393 (2001).
5. K. H. Kim, C. Buehler, and P. T. C. So, "High-speed, two-photon scanning microscope," Appl. Opt. **38**(28), 6004–6009 (1999).
6. A. H. Buist, M. Muller, J. Squier, and G. J. Brakenhoff, "Real-time two-photon absorption microscopy using multipoint excitation," J. Microsc. **192**(2), 217–226 (1998).
7. J. Bewersdorf, R. Pick, and S. W. Hell, "Multifocal multiphoton microscopy," Opt. Lett. **23**(9), 655–657 (1998).
8. S. W. Hell and V. Andresen, "Space-multiplexed multifocal nonlinear microscopy," J. Microsc. **202**(3), 457–463 (2001).
9. D. Fittinghoff, P. Wiseman, and J. Squier, "Widefield multiphoton and temporally decorrelated multifocal multiphoton microscopy," Opt. Express **7**(8), 273–279 (2000).
10. T. Nielsen, M. Fricke, D. Hellweg, and P. Andresen, "High efficiency beam splitter for multifocal multiphoton microscopy," J. Microsc. **201**(3), 368–376 (2001).
11. D. Oron, E. Tal, and Y. Silberberg, "Scanningless depth-resolved microscopy," Opt. Express **13**(5), 1468–1476 (2005).
12. G. Zhu, J. van Howe, M. Durst, W. Zipfel, and C. Xu, "Simultaneous spatial and temporal focusing of femtosecond pulses," Opt. Express **13**(6), 2153–2159 (2005).
13. M. E. Durst, G. Zhu, and C. Xu, "Simultaneous spatial and temporal focusing for axial scanning," Opt. Express **14**(25), 12243–12254 (2006).
14. H. Dana and S. Shoham, "Remotely scanned multiphoton temporal focusing by axial grism scanning," Opt. Lett. **37**(14), 2913–2915 (2012).
15. R. Du, K. Bi, S. Zeng, D. Li, S. Xue, and Q. Luo, "Analysis of fast axial scanning scheme using temporal focusing with acousto-optic deflectors," J. Mod. Opt. **56**, 99–102 (2008).

#246643 Received 23 Jul 2015; revised 28 Aug 2015; accepted 3 Sep 2015; published 8 Sep 2015

16. A. Straub, M. E. Durst, and C. Xu, "High speed multiphoton axial scanning through an optical fiber in a remotely scanned temporal focusing setup," Biomed. Opt. Express **2**(1), 80–88 (2011).
17. B. F. Grewe, F. F. Voigt, M. van 't Hoff, and F. Helmchen, "Fast two-layer two-photon imaging of neuronal cell populations using an electrically tunable lens," Biomed. Opt. Express **2**(7), 2035–2046 (2011).
18. F. O. Fahrbach, F. F. Voigt, B. Schmid, F. Helmchen, and J. Huisken, "Rapid 3D light-sheet microscopy with a tunable lens," Opt. Express **21**(18), 21010–21026 (2013).
19. E. J. O. Hamel, B. F. Grewe, J. G. Parker, and M. J. Schnitzer, "Cellular level brain imaging in behaving mammals: an engineering approach," Neuron **86**(1), 140–159 (2015).

1. Introduction

Since the advent of two-photon excited fluorescence (TPEF) microscopy [1], efforts have been made to increase its imaging speed. In a typical TPEF microscope, image is obtained by raster-scanning the laser beam across the focal plane, and 3D image stacks are collected by moving the focal plane along the optical axis. Although high-speed scanners, such as resonant scanners and polygonal mirrors [2–5], have been employed in many laser scanning microscopies, the mechanical scanning process limits the ultimate frame rate to 100s Hz. Other alternative methods such as multi-foci using a lenslet [6–8] or beamsplitter array [9,10] to achieve high frame rate work at the expense of lowering the resolution and increasing the complexity of the microscope system.

The limit of imaging speed is largely resolved by a disruptive imaging technique, i.e. temporal focusing microscopy or simultaneously spatial temporal focusing (SSTF) microscopy, proposed in 2005 [11,12]. Unlike conventional TPEF microscopes that spatially focus the laser beam to a single point, a temporal focusing microscope achieves high photon density by temporally narrowing the laser pulse into a thin "light sheet" of 3-5 μm in thickness. Since the entire focal plane is illuminated simultaneously, no scanning process is required for the temporal focusing microscope, and thus the imaging speed is theoretically equivalent to the repetition rate of a pulsed laser. Practically, the imaging speed is limited by the refreshing rate of the photodetector, e.g., EMCCD camera has a refreshing rate of up to ~1 kHz.

Although a temporal focusing microscope can rapidly collect 2-D cross-sectional images, it still relies on mechanical scanning to obtain 3-D image stacks. In other words, either the objective lens or the sample, e.g., anaesthetized mouse or zebrafish, needs to be affixed to a precision stage and scanned along the optical axis, which is slow and can induce unwanted vibration and motion artifacts when the scanning speed is high, e.g., 10 Hz. Due to these drawbacks, new remote scanning methods have been developed. These methods are mostly related to the modulation of group velocity dispersion (GVD). For example, GVD can be modulated via prisms [13,14], acousto-optic deflectors [15] or piezo bimorph mirror [16]. Although axial scanning via GVD modulation achieves high speed, e.g., 10s kHz, they all have an issue that the acquired images will be blurred when the temporally focused imaging plane scans away from the original focal plane of the detection optics [14], which limits the application of large volume scanning.

To solve the aforementioned problem, we develop a new temporal focusing microscope by adopting an electrically tunable lens (ETL) as the remote axial scanning device, which ensures the coincidence of the scanning plane of the illumination optics and the focal plane of the detection optics. The focal power (or focal length) of an ETL can be electrically tuned by applying different currents; it has been used to perform fast axial scanning in conventional two-photon microscopes and light-sheet microscopes [17,18]. In the following sections, we will demonstrate that by properly incorporating the ETL into a wide-field temporal focusing microscope, high-speed (up to 1 kHz) and large-depth (100 μm with a 60 × objective) two-photon fluorescence imaging can be achieved.

2. Microscope design

Figure 1 presents the schematic of the custom-built wide-field temporal focusing microscope. The core components include a Ti-Sapphire regenerative amplifier (Spectra-Physics, Spitfire Pro; pulse width: 100 fs; repetition rate: 1 kHz), a 1200 lines/mm grating (Thorlab, USA), an

#246643 Received 23 Jul 2015; revised 28 Aug 2015; accepted 3 Sep 2015; published 8 Sep 2015

objective lens (Nikon Fluor 60 × 1.00NA), an EMCCD camera (ProEM, Princeton Instrument, USA) and an electrically tunable lens (EL-10-30-Ci-VIS-LD-MV, Optotune, Switzerland).

In Fig. 1, the output beam from the laser amplifier is first sent to a half-wave plate and a polarizer to adjust its polarization and accordingly power; then, the laser beam is spatially dispersed via a blazed grating; the incident angle of the laser beam is adjusted so that the optical spectrum's central frequency aligns with the optical axis. After that, the dispersed laser beam is collected by a collimating lens (f_c = 500mm), followed by a set of relay lens (f_{r1} = 300mm, f_{r2} = 200mm) to adjust the beam size so that it will fill the back aperture of the objective lens. At the focal plane of the objective lens, the dispersed spectrum of the laser beam recombines and thus a temporally focused ultrashort pulse is reproduced, generating a high photon-density "light sheet" for two photon excitation.

Axial scanning of the focal plane is performed by the ETL, which is positioned 15 mm behind the objective lens, shown in Fig. 1. The ETL consists of a shape-changing elastic membrane and a concave offset lens (f_{offset} = −150mm). When an electrical current (0 ~270 mA) is applied to it, the focal power of the ETL can be tuned from −2 to 6 diopter, and hence effectively modulating focal plane of the microscope system.

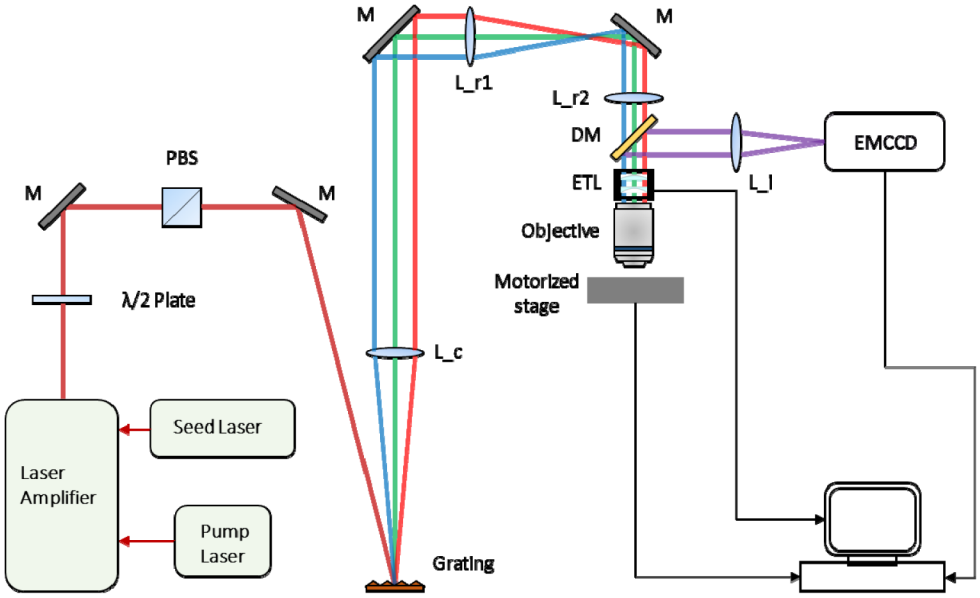

Fig. 1. Schematic of the fast 3-D temporal focusing microscope. M: mirror; PBS: polarization beam-splitter; DM: dichroic mirror; ETL: electrically tunable lens; L_c: collimating lens f_c = 500mm; L_r1: first relay-lens f_{r1} = 300mm; L_r2: second relay-lens f_{r2} = 200mm; L_i: imaging lens (zoomlens, Canon);

3. Evaluation of optical performance

In this section, we present the evaluation of the temporal focusing system including the (1) focal plane scanning via the ETL, (2) the associated the magnification variation, and (3) the point spread function (PSF) measurement in both lateral and axial directions with ETL. It may be observed in Fig. 1 that the ETL is shared by both the detection light path (purple line: objective – EMCCD) as well as the illumination path (red line: laser – objective). Accordingly, based on the reversibility of light, the detected images should remained in focus on the EMCCD no matter how the ETL tunes the focal plane. This becomes clear if we consider the combination of the ETL and objective lens as a new objective lens. To verify this, we scanned the pollen sample (~40 μm thick) along the optical axis using both a

#246643 Received 23 Jul 2015; revised 28 Aug 2015; accepted 3 Sep 2015; published 8 Sep 2015

motorized stage and the ETL and compared the results, shown in Fig. 2. In Fig. 2, the top and bottom row show the cross-sectional images of pollen samples scanned by the motorized stage and the ETL respectively. As expected, no blurry images are found in the results collected by the ETL when scanning through a 40 μm-thick pollen sample; we also find the image quality of the ETL comparable with those obtained by the motorized stage.

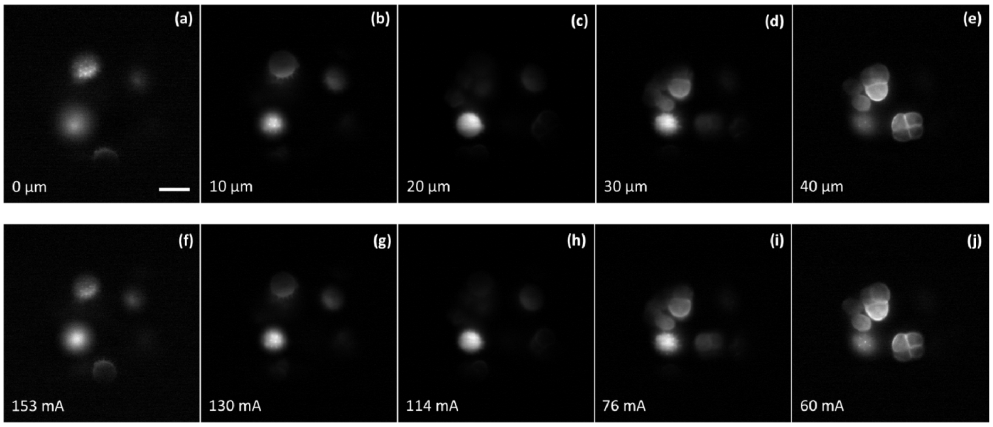

Fig. 2. Two-photon fluorescence images of pollen samples obtained at different depths: (a)-(e) images scanned by a motorized stage from 0~40 μm, and (f)-(j) images scanned by tuning the ETL. Note the slight change of magnification (or the field of view size). Scale bar = 20μm.

For practical scanning applications, we must precisely correlate the axial shift of focal plane with the ETL current input in order to obtain the depth information of individual optical cross-sections for 3-D reconstruction. In addition, since the temporal focusing microscope is not a telecentric optical system, any focal length-tuning induced by the ETL will slightly affect the system magnification, i.e. size of field-of-view. Accordingly, we must identify the relationship between the magnification and focus-tuning. Finally, the relationship between the temporal-focusing sectioning quality, i.e. lateral and axial resolution, and the focal plane scanning (or ETL current) needs to be investigated. This is important because the effective numerical aperture (NA) of the objective lens will vary when the focal length of the ETL is tuned, thereby affecting the imaging resolution; also, shifting the focal plane may negatively affect the aberration correction capability of the microscope objective in the transverse and longitudinal fields [10].

To correlate the scan depth and ETL current input, we measured the TPEF(z) traces by scanning a spin-coated Rhodamine-6G film sample using a motorized stage, where TPEF(z) refers to the total two-photon fluorescence signal of the captured image at different axial position along the z-axis. Position of the focal plane with maximum fluorescence intensity was then recorded at different ETL-current values. Figure 3(a) and 3(d) show the focal plane scanning as a function of the ETL current input, achieving a 100 μm scan range for a 60 × objective lens (NA = 1.0; WD = 2 mm). The results also indicate that larger ETL currents shift the focal plane towards the objective, while smaller currents shift the focal plane away from the objective lens. Note that the zero position, i.e. no axial shift in reference to the system without the ETL, is defined at 75 mA in these experiments.

For quantifying the effect of magnification variation, we imaged a pollen grain at different ETL-currents and directly measured the magnification change from the image sequence. Figure 3(b) presents the results, where the magnification variation is normalized with the image at the original focal plane (ETL-current = 75mA). From the results, we find that the image magnification decreases with increasing ETL drive current.

To investigate the imaging resolution affected by the ETL, the PSF(x, y, z), or Full Width Half Maximum (FWHM), of the temporal focusing system was measured using 200 nm fluorescent beads; the results are shown in Fig. 3(c). From Fig. 3(c), we find that the

#246643 Received 23 Jul 2015; revised 28 Aug 2015; accepted 3 Sep 2015; published 8 Sep 2015

resolution decreases with increasing ETL currents, which is mainly caused by the decrease of NA as the focal plane is shifted away from the objective lens. When the focal plane is shifted toward the objective lens, the aberration degradation becomes more dominant than the increase of NA, setting a limit for the imaging resolution [10]. Considering the change of imaging resolution within large axial scan range, we recommend the ETL to be operated from 0 to 235 mA, corresponding to a resolution change from about 6 to 9 μm in the axial direction and 1.07 to 1.44 μm in the lateral direction. It is worthwhile to note that in the experiments, we slightly underfill the back aperture of objective lens at the zero position (ETL current = 75mA) in order to prevent overfilling the back aperture when the ETL is driven below 75mA.

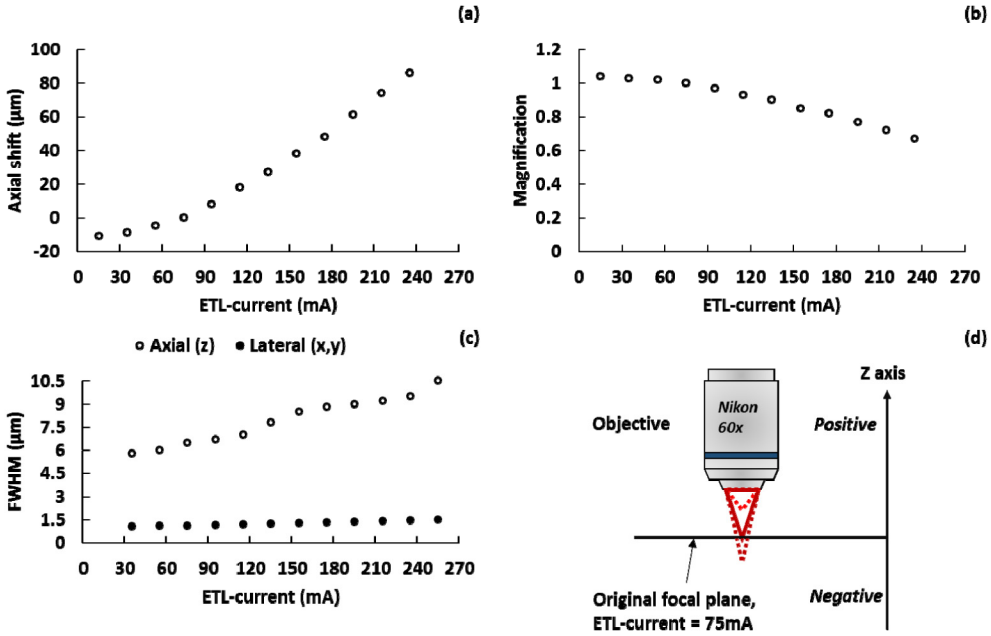

Fig. 3. (a) Relationship between the axial shift of focal plane and the ETL current input; (b) relationship between the image magnification and the ETL current input; (c) point-spread-function (PSF) measurement along lateral and axial (z axis) directions as a function of the ETL current input; (d) illustration of the axial (focal plane) scanning, where positive values refer to a decrease in working distance and vice versa.

In order to reason the results above, we develop a model for the temporal focusing microscope based on geometric optics. Figure 4 shows the schematic of the model, where the ETL and the objective lens are treated as thin lenses; P is the intermediate imaging plane of the grating, which will be imaged to the focal plane, i.e. the temporal focusing plane.

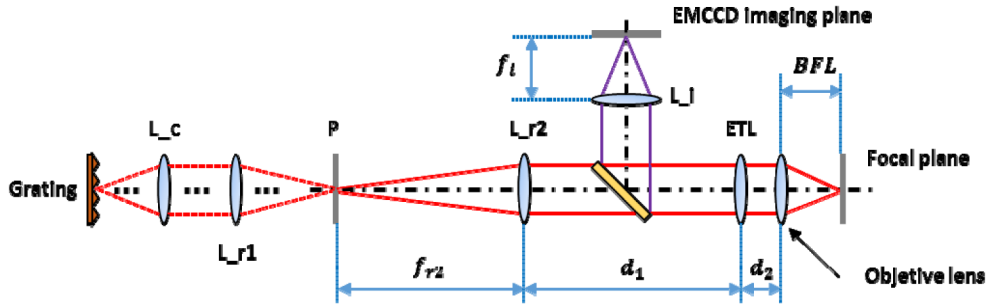

Fig. 4. Optical model of the temporal focusing microscope. Note the optical path from the grating to P is omitted. P is the intermediate imaging plane of the grating, and BFL refers to the back focal length of the ETL and the objective lens.

#246643 Received 23 Jul 2015; revised 28 Aug 2015; accepted 3 Sep 2015; published 8 Sep 2015

Expression for the back focal length (BFL), image magnification ($M_{imaging}$) and field of view (FOV) can be obtained by applying thin lens equation as follows:

$$BFL = \frac{f_o}{1 + \frac{f_o}{f_{ETL} - d_2}}$$

$$M_{imaging} = \frac{f_i}{f_o} \times (\frac{d_2 - f_o}{f_{ETL}} - 1)$$

$$FOV = D\frac{f_c}{f_{r1}} M_{illumination} = D\frac{f_c}{f_{r1}} \frac{1}{M_{imaging}} \frac{f_i}{f_{r2}}$$

where f_o is the focal length of the objective lens; D is the laser beam diameter on the grating; and $M_{illumination}$ is the magnification of the optical system from P to the focal plane.

From the ETL datasheet, we know that the focal power of the ETL, i.e. 1/ f_{ETL}, is proportional to the ETL current input (I_{ETL}). Accordingly, as the ETL current increases, the BFL and the imaging magnification will decrease, which is consistent with the measured data presented in Fig. 3(a) and 3(b).

The numerical aperture (NA) of the optical system is related to the laser beam size at the back aperture of the objective lens, which can be expressed as:

$$NA \propto a \times (1 - \frac{d_2}{f_{ETL}})$$

where a is the beam size at the back aperture of the objective lens when ETL-current = 75mA. Accordingly, as the ETL current increases, f_{ETL} will decrease and thus the NA decreases. This trend is consistent with the measured data presented in Fig. 3(c). (Detailed analyses of NA using ZEMAX can be found in [10].)

4. In-vivo imaging of zebrafish brain

To demonstrate the capability of our temporal-focusing microscope, we imaged zebrafish *in vivo* containing the transgene tg(Elval3:GCaMP6f), a calcium (Ca^{2+}) reporter line expressed in the brain and spinal cord. Zebrafish larvae approximately 3-5 days post fertilization were paralyzed using tubocurarine (100 μM, Sigma-Aldrich), a muscle relaxant, and mounted in 1% low melt agarose. All zebrafish was mounted dorsally to expose both hemispheres of the brain.

In the experiment, volumetric two-photon imaging was performed at the brain region, as shown in Fig. 5(a) indicated by red circle, at a speed of 5Hz by applying a triangular-wave drive current (2.5Hz, peak to peak: 75mA - 155mA) to the ETL. To capture a single 2-D frame with the EMCCD camera, we set the exposure time to be 10 ms (100 Hz in terms of speed). The results are shown in Fig. 5(b)–5(h); the z position of each image, as well as its corresponding magnification were calculated using the data presented in Fig. 3(b) and 3(c). For a temporal focusing microscope, the optical cross-sections captured in Fig. 5(a)–5(i) show satisfying results with individual neurons and micro-scale structures clearly identifiable at different depths. In addition, the images were collected at low laser power (60 mW / 3000 μm^2), introducing negligible heat effect to the brain of zebrafish. (The laser will induce permanent damage to the zebrafish brain at a power level ~200 mW/3000 μm^2.)

It is worthwhile to note that although the results in this paper were obtained at 5 Hz for quality images, the ETL can practically scan the focal plane at a speed of up to 1 kHz, generating 3-D volumetric images. The high-speed scanning capability and applications of the ETL has been verified and reported in previous works [17, 18]. Compared with traditional laser-scanning two-photon microscopes, our wide-field setup is easier to implement and not

#246643 Received 23 Jul 2015; revised 28 Aug 2015; accepted 3 Sep 2015; published 8 Sep 2015

subjected to the photon-limited tradeoffs between the FOV, the temporal resolution, i.e. speed, and the "d" values, i.e. detection fidelity [19], making it a promising imaging tool for studying neuroscience.

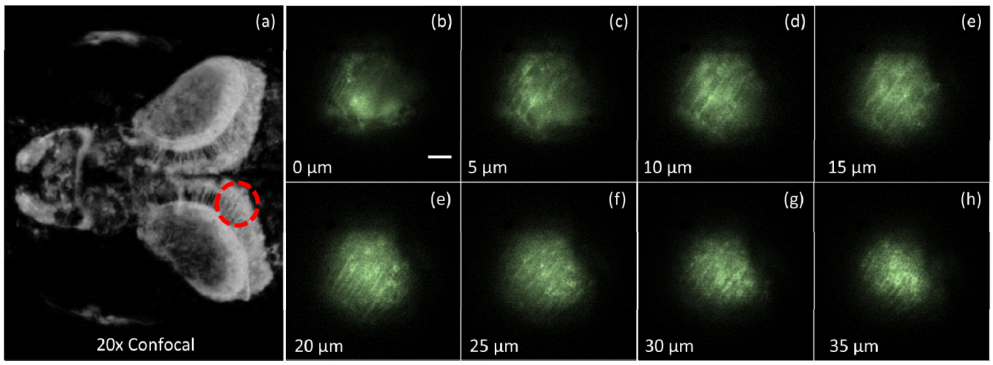

Fig. 5. In-vivo two-photon Ca^{2+} imaging of zebrafish. Left: image of a 4dpf larva zebrafish head obtained by a confocal microscope. The red circle indicates a zoom-in area imaged using the temporal focusing microscope. Right: (b) - (h) fluorescence images from the temporal focusing microscope of the 4dpf zebrafish larva brain at different depths; the z position of each image is obtained by Fig. 3(b); and the magnification is re-scaled using Fig. 3(c); scale bar = 20 μm; pixels: 256 × 256. Images were collected in the left hemisphere of the tectum opticum.

5. Summary

In this work, we present a temporal focusing microscope integrated with an electrically tunable lens for fast 3-D *in vivo* two-photon imaging. Compared with other non-mechanical axial scanning methods, e.g., GVD modulation, our design enables large-depth (100 μm) and high-speed z-scanning (up to 1 kHz) without the image blurring issue. This is achieved by the ETL which ensures the coincidence of the scanning plane and focal plane of the detection optics. The performance of the temporal focusing microscope was characterized and carefully evaluated including the ETL-enabled z-scanning, the associated the magnification variation, and the optical cross-sectioning capability. Lastly, an *in vivo* Ca2 + imaging experiment on GCaMP6 labeled zebrafish brain was designed and performed to demonstrate the optical cross-sectioning capability of the system, imaging a dense neural region in the midbrain called the tectum opticum. Upon imaging, the electrically tunable lens exhibited comparable results with mechanical scanning systems often used in confocal microscopes. The high-speed nature of the temporal focusing system makes it suitable for studying neural signaling events. In the future, we will use the system to image neuronal dynamics in the zebrafish brain *in vivo* via voltage indicators.

Acknowledgments

This work is partially supported by the HKSAR Innovation and Technology Commission (ITC) Innovation and Technology Fund (ITF), ITS/094/13FP, the Shun Shing Institute of Advanced Engineering of the Chinese University of Hong Kong, Project #BME-p1-14, HKSAR Research Grants Council, General Research Fund, Project # 439813, and the Lui Chee Woo Institute of Innovative Medicine Fund.